ON THE TRACKING OF SPACE OBJECTS USING AURORAL IMAGES

G. Borderes Motta(1), T. Sergienko(1), D. Kastinen(1), U. Brandstrom(1), Lars-Henrik Snow(1), J. Kero(1), H. Sundberg(2), S. Barra(2), J. Ask(2), and P. Hyvönen(2)

(1)Swedish Institute of Space Physics, 1234 Kiruna, Sweden, Email: {gabriel.borderes.motta, tima.sergienko, daniel.kastinen, urban.brandstrom, lars-henrik.snow, kero}@irf.se
(2)Swedish Space Corporation, 171 04 Solna, Sweden, Email: {hanna.sundberg, stefano.barra, jacob.ask, petrus.hyvonen}@sscspace.com

ABSTRACT

ALIS_4D is a recently upgraded version of the Auroral Large Imaging System (ALIS) - a wide-field optical system with imagers operating in the visible and near-infrared regions. ALIS_4D aims to support research on light phenomena in the upper atmosphere, such as northern lights. It can monitor a large part of the sky with overlapping fields of view from different stations. In this context, we raise the following questions: Can we use ALIS_4D to identify and determine the orbit of space objects? What can be the main contributions of ALIS_4D to the space debris tracking framework? How should an ALIS_4D campaign for such a proposal be scheduled and executed? Aiming to answer these questions, we developed an algorithm to identify space object traces and compute their orbits. Considering the geometry, visibility, and filters used, we choose a set of images to apply the algorithm. Data analysis showed that it is possible to determine a satellite's orbits using ALIS_4D. To verify the algorithm, we compared the orbital elements of the object tracked with ALIS_4D with known space debris catalogs.

Keywords: ALIS_4D; Satellites; Space Debris; Tracking.

1. INTRODUCTION

The growth of the space debris population imposes a threat to the space environment. In this context, monitoring these objects for planning action and avoiding collisions becomes a challenge in space engineering. In such a context, a question arises: Can observation instruments dedicated to other goals be adapted to contribute to space monitoring?

In this work, we explore the possibility of using ALIS_4D, an optical system for studies on northern lights, to track and determine the orbit of space objects.

2. THE AURORAL LARGE IMAGING SYSTEM AND ALIS_4D

The Auroral Large Imaging System (ALIS) operated in its first version from 1993 to 2019. Up to eight remotely-controlled stations operated by IRF (see Figure 1) in Northern Sweden composed the ALIS. Each station had a highly scientific CCD detector and a filter wheel with space for six narrow-band interference filters. The system reached exciting research results:

- The first unambiguous observations of Radio-Induced Optical Emissions (RIOE, stimulated by the so-called EISCAT Heating facility, sometimes called "artificial aurora") at high latitude [1];
- the first 3D-reconstruction of radio-induced optical emissions [2];
- the first ground-based day-time auroral images [3];
- observation of water in a Leonid meteor-trail [4];
- first unambiguous observations of radio-induced N_2^+ emission (4278 Å, "blue" auroral line) [5];
- the first and unexpected observation of radio-induced optical emissions when transmitting in extraordinary wave-mode [6].

The four stations that were used in this study, Abisko (A), Kiruna-knutstorp (K), Silkkimuotka (S), and Tjautjas (T), are displayed in Figure 1.

In 2019, ALIS_4D replaced ALIS by upgrading the stations with EMCCD imagers combining high time resolution ($\geq$ 25 images/), good spatial resolution (ca. 750 m at 100 km altitude) with possibility of almost continuous imaging with overlapping fields-of-view from several stations.

Proc. 2nd NEO and Debris Detection Conference, Darmstadt, Germany, 24-26 January 2023, published by the ESA Space Safety Programme Office
Ed. T. Flohrer, R. Moissl, F. Schmitz (http://conference.sdo.esoc.esa.int, February 2023)

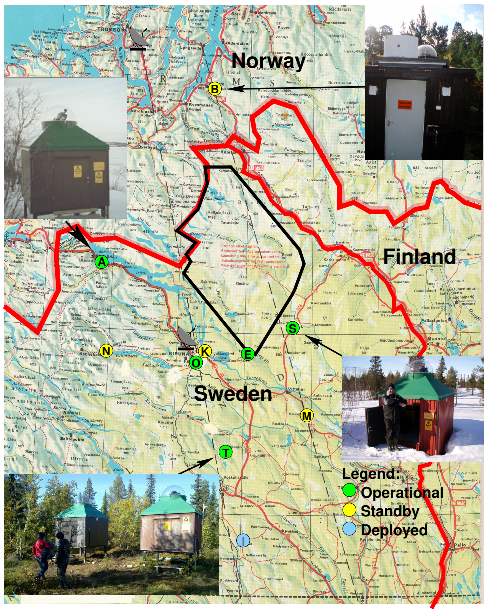

Figure 1. ALIS_4D map. Stations used in this study were: Abisko (A), Kiruna-knutstorp (K), Silkkimuotka (S) and Tjautjas (T). ESRANGE (E) was not available during this study. ([8])

3. FEATURES OF OBSERVATIONS AT HIGH LATITUDES

One of the most peculiar characteristics of the observation using ALIS_4D is geographical position, i.e., the high latitude where the station is. Observers in very high latitudes (or very low) have more time to observe space objects (see Figure 2).

On the other hand, space objects in low inclination do not enter into the field of view of observation at high latitudes. Figure 3 shows the space objects by their size plot in semi-major axis and inclination and the regions where these objects are visible in Abisko. One can note that most of these objects are visible.

Objects with highly inclined orbits are visible from latitudes close to zero, but this only can be done when the space object crosses the equator plane at sunrise or sunset local time. Such a condition restricts the number of debris and satellites visible in high orbital inclination.

4. DATA ANALYSES

Two of the ALIS_4D filters make it able to observe space objects. Considering this issue, we performed a campaign on April 1, 2020, from 19:49 to 20:58. The data used in the present work were taken during this campaign. Figure 4 shows one of the images taken during the campaign by Kiruna-knutstorp station at 19:49. The data set files contain one minute of capture in a pack of 116 frames.

4.1. Radon Transform

The first step of our analyses is filtering the data. For each file, we subtract each frame from its consecutive one. Therefore, we convolute frames with a constant matrix, remove weak signals and sum all frames. The result of this process is on panel "A)" of Figure 5, in which two traces of space objects are in evidence.

After this we apply a two-dimensional Radon transform (panel "B)" of Figure 5). A Radon transform is a line integral transform from a function on the plane to another function on space of lines in the plane. Considering the traces of space objects have shape of line on the domain, their pixels creates a peak of intesity on the image. We select the 20 peaks of intensity in the Radon transform. After we convert the peaks in lines (panel "C)" of Figure 5), one can note that two of these lines match with the traces.

The next step is to differentiate the lines in positive and false positive detection. We set a rectangle cut around the line on the image to analyze it. We extract the data inside the rectangle and sum the pixels in lines perpendicular to the line computed by the Radon transform. After joining all frames, we can get a two-dimensional image. The image is in the middle of Figure 6.

4.2. Second Radon Transform

We divided the images extracted from each line into packs of frames. Furthermore, we applied the Radon transform to the result. Figure 6 shows this process. From each Radon transform, we compute the highest peak.

We plot the magnitude of the peaks (see Figure 7). In this plot, the lines with stronger signals are the ones that match the trace.

Finally, we can extract the pixel of the trace using the line (see Figure 8).

4.3. Image Segmentation

We used the described procedure on all images of the campaign. Further, the data analysis presented issues related to the Radon transform convergence. For example, the photo captured at 19:51 UT (see Figure 9) has a trace close to the border of the image file that does not match the lines arising from the Radon transform.

The next step is to divide the image into smaller pieces to avoid non-convergence. Therefore, we apply the Radon transform to each image piece and back to the previous procedure.

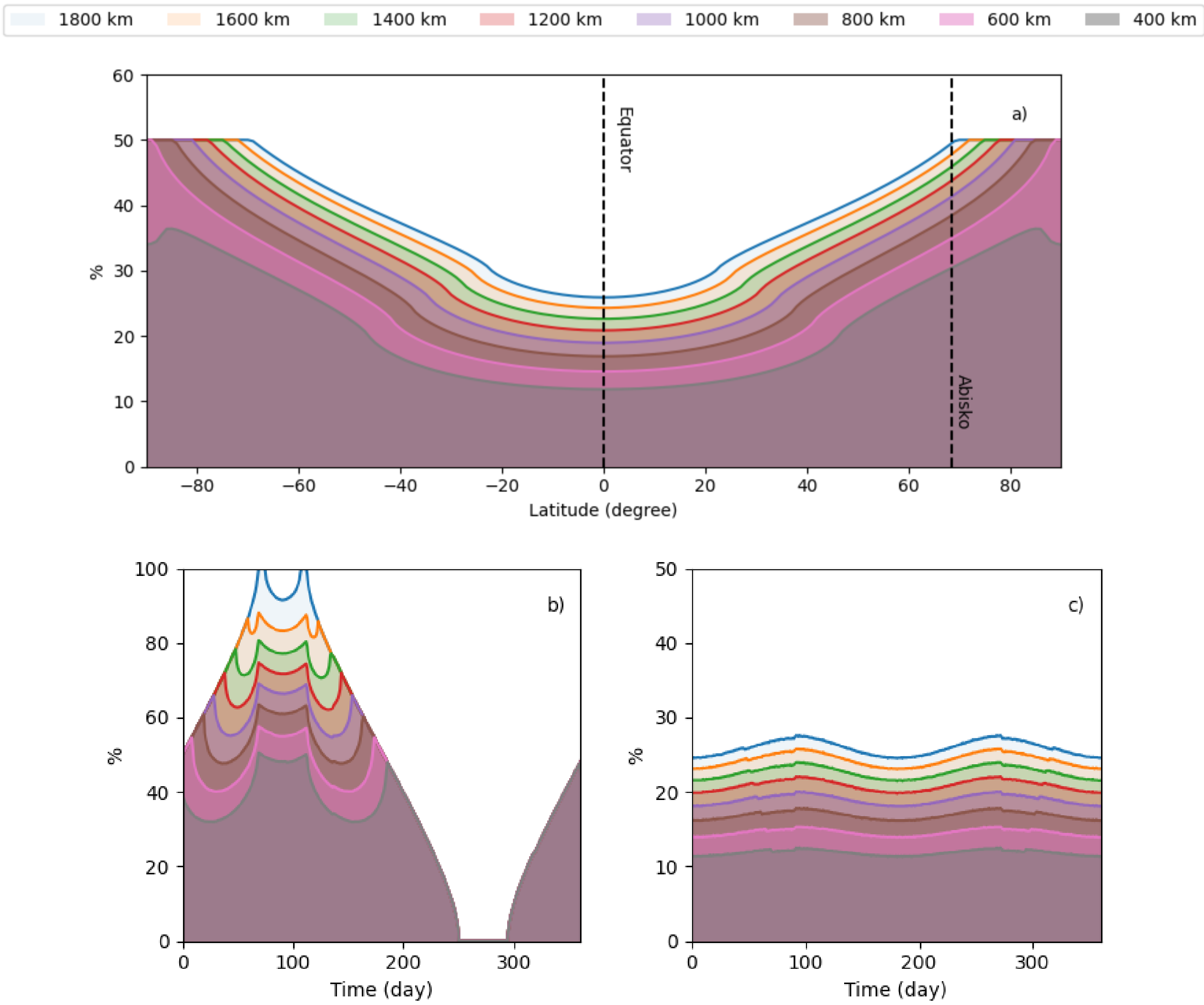

Figure 2. Potential time of space object observation for different altitudes. Panel "a)" shows the percentage of the year for space object observation for different latitudes (y-axis). The percentage of each day for a complete year cycle(y-axis) of observation from Abisko (panel "b)") and from equator (panel "c)")

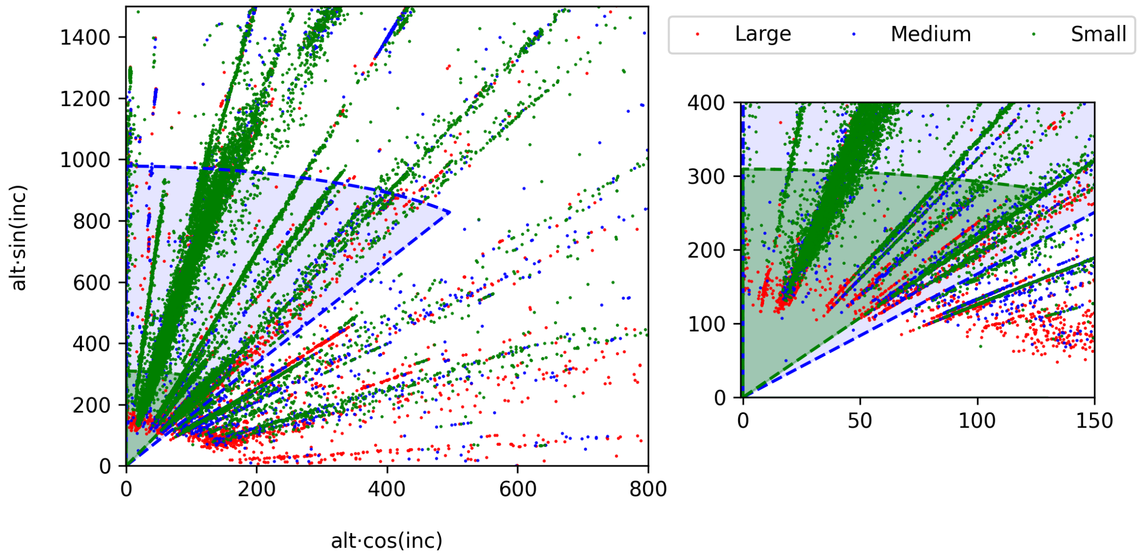

Figure 3. Sample of space objects characterized by size ([8]). The green region defines the region where small space objects (cross-section $< 0.1m^2$*) are visible by the naked eye at Abisko latitude, and the blue region is the same for medium size space objects* $(0.1m^2 < cross - section < 1m^2)$*.*

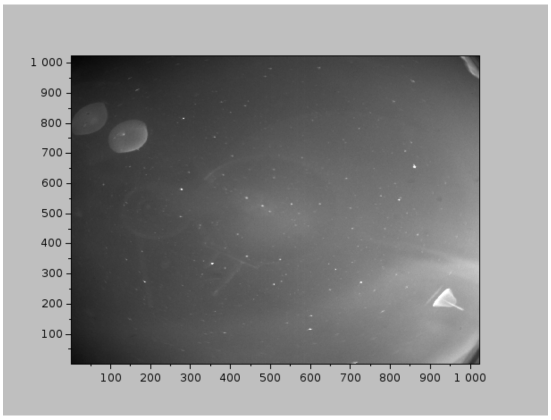

Figure 4. Image of 1 min taken by Kiruna-knutstorp station in 2020-04-01 at 19:49 UT.

5. FINAL REMARKS

We have shown the procedure we are developing to identify traces of space objects in ALIS_4D data. Our main goal is to automatize the process of track and obit determination aiming to use ALIS_4D to contribute to the space awareness scenario.

ACKNOWLEDGMENTS

The project was financed by Swedish National Space Agency, under the NRFP-4 program, called "ALIS_4D AUTO-SSA", diary number 2020-304. It is also partly funded by the EU project RIT (Rymd för innovation och tillväxt/Space for innovation and growth) with the objective of developing the space region in northern Sweden.

REFERENCES

1. Brändström B. U. E., Leyser T. B., Steen Å., Rietveld M. T., Gustavsson B., Aso T., Ejiri M., (1999). *Unambigous evidence of HF pump-enhanced airglow*, Geophys. Res. Lett., **26**(23), 3561–3564.
2. Gustavsson B., Sergienko T., Rietveld M. T., Honary F., Steen Å., Brändström B. U. E., Leyser T. B., Aruliah A. L., Aso T., Ejiri M., Marple S., (2001). *First Tomographic estimate of volume distribution of volume distribution of HF-pump enhanced airglow emission*, J. Geophys. Res., **106**(A12), 29105–29123.
3. Rees D., Conde M., Steen Å., Brändström U., (2000). *The first daytime Ground-Based Optical Image of the Aurora*, Geophys. Res. Lett., **27**(3), 313–316.
4. Pellinen-Wannberg A., Murad E., Gustavsson B., Brändström U., Enell Carl-Fredrik, Roth C., Williams I. P., Steen Å, (2004). *Optical observations of water in Leonid meteor trails* Geophys. Res. Lett., **31**.
5. Gustavsson B., Leyser T. B., Kosch M., Rietveld M. T., Steen Å, Brändström B. U. E., Aso T., (2006). *Electron Gyroharmonic Effects in Ionization and Electron Acceleration during High-Frequency Pumping in the Ionosphere*, Phys. Rev. Lett., **97**, 195002.
6. Blagoveshchenskaya N. F., Borisova T. D., Kosch M., Sergienko T., Brändström U., Yeoman T. K., Häggström I, (2014). *Optical and ionospheric phenomena at EISCAT under continuous X-mode HF pumping*, J. Geophys. Res., **119**(12).

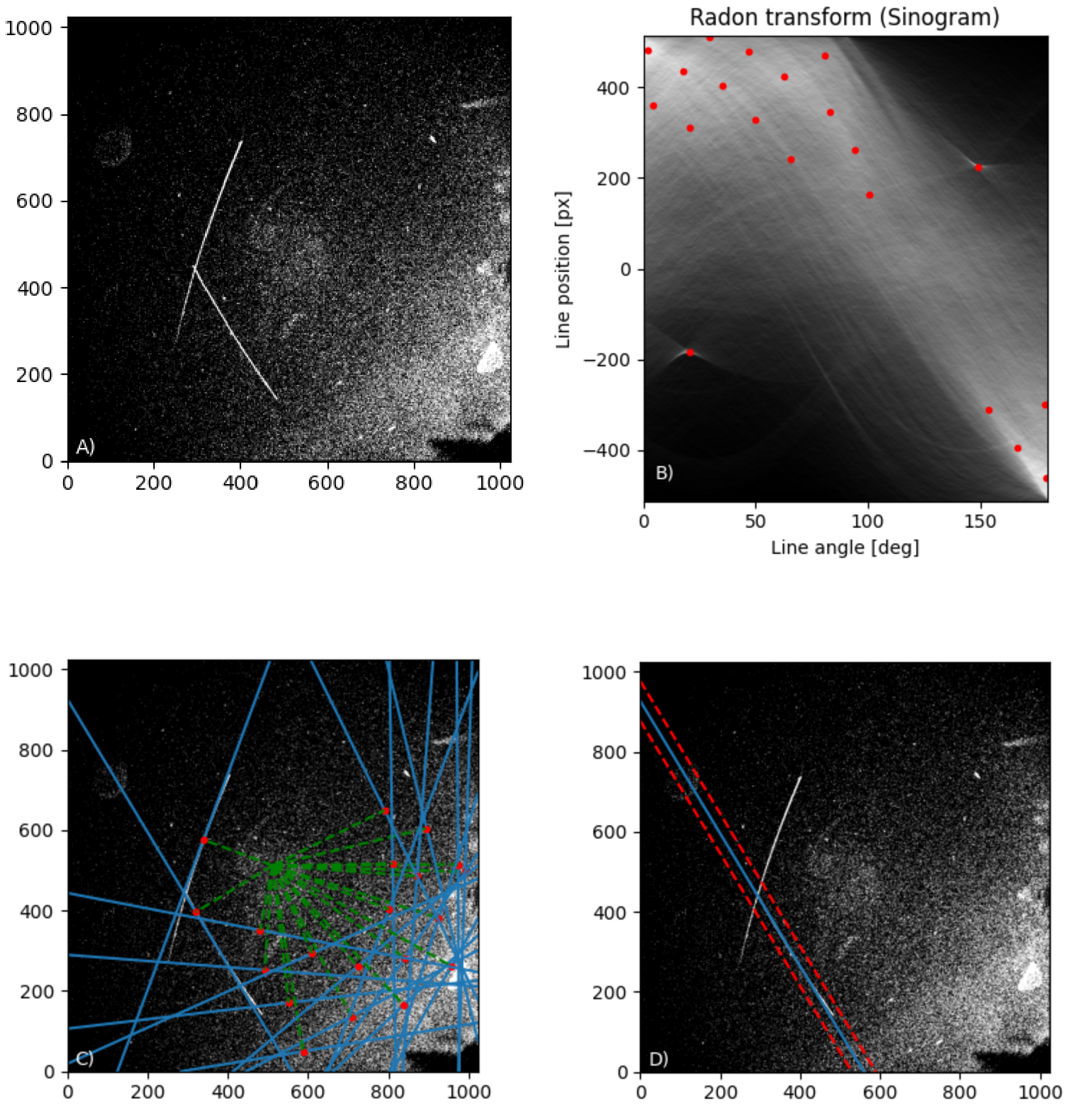

Figure 5. Panel A): Image captured at 19:49 UT and filtered. Panel B): Radon Transform of panel A with 20 peaks selected. Panel C): Original image with the 20 lines identified by the peaks of the Radon transform. Panel D): Representation of the cut we intend to further analyse by expanding in the time dimension.

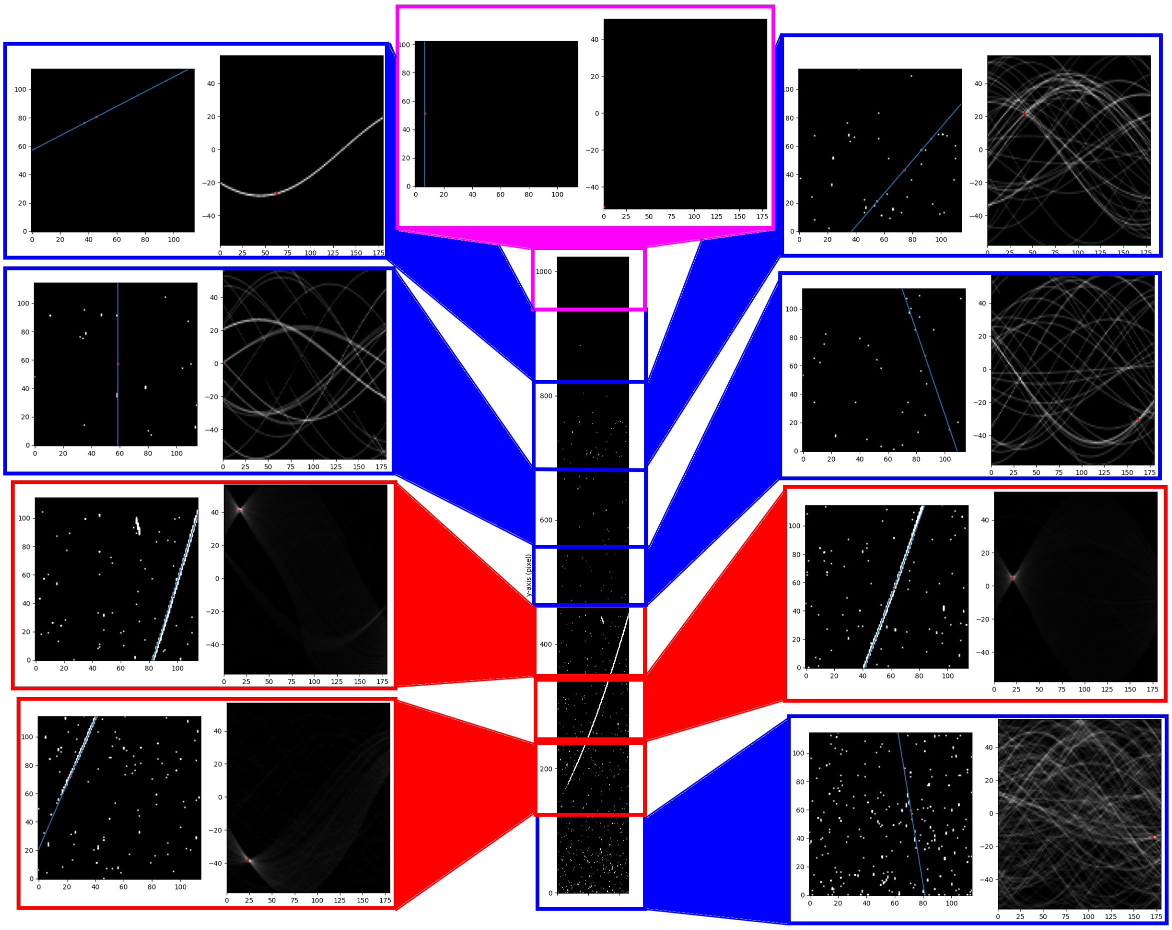

Figure 6. Image of one line in the dimensions of the line vs. the frame. Around the images are the cuts and the respective Radon transform.

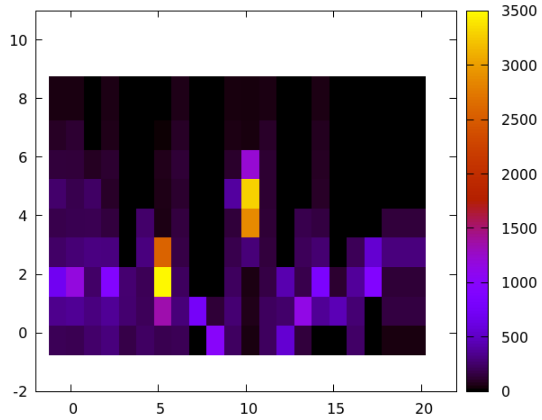

Figure 7. Magnitude of the peaks, x-axis is the line extract from the first Radon transform in sequence and y-axis is the piece of the image extracted from each line.

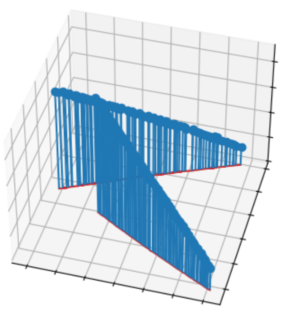

Figure 8. Traces extracted from the original image in Figure 4.

7. Brändström, U.,Hyvönen, P., Kastinen, D., Kero, J., Sergienko, T., (2022). *ALIS_4D NRFP3 Report*.
8. CATALOG: Space-Track.org's Application Programming Interface (API). https://www.space-track.org/

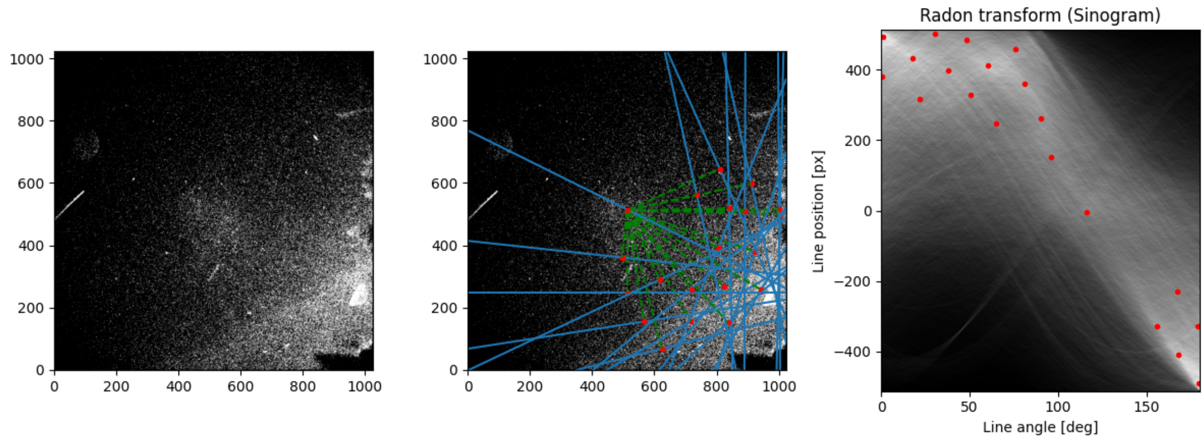

Figure 9. Left panel: Image taken by the Kiruna-knutstorp station on 2020-04-01 at 19:51 UT. Middle panel: Image with the 20 lines computed from the peaks. Right panel: Radon transform from the image with the 20 peaks.